HHS Public Access

Author manuscript

Biochemistry. Author manuscript; available in PMC 2021 June 09.

Published in final edited form as:

Biochemistry. 2020 June 09; 59(22): 2078–2088. doi:10.1021/acs.biochem.0c00084.

UbcH5 Interacts with Substrates to Participate in Lysine Selection with the E3 Ubiquitin Ligase CHIP

Adam Kanack[1,2], **Vinayak Vittal**[3], **Holly Haver**[4], **Theodore Keppel**[1], **Rebekah L. Gundry**[1,5], **Rachel E. Klevit**[3], **Kenneth Matthew Scaglione**[1,2,4,6,7,*]

[1]Department of Biochemistry, Medical College of Wisconsin, Milwaukee, WI 53226, USA

[2]Neuroscience Research Center, Medical College of Wisconsin, Milwaukee, WI 53226, USA

[3]Department of Biochemistry, University of Washington, Seattle, WA 98195, USA

[4]Department of Molecular Genetics and Microbiology, Duke University, Durham, NC 27710, USA

[5]Current Address: CardiOmics Program, Center for Heart and Vascular Research; Division of Cardiovascular Medicine; and Department of Cellular and Integrative Physiology, University of Nebraska Medical Center, Omaha, NE, 68198, USA

[6]Department of Neurology, Duke University, Durham, NC 27710, USA

[7]Duke Center for Neurodegeneration and Neurotherapeutics, Durham, NC, 27710, USA

Abstract

The E3 ubiquitin ligase C-terminus of Hsc70 interacting protein (CHIP) plays a critical role in regulating the ubiquitin-dependent degradation of misfolded proteins. CHIP mediates the ubiquitination of the alpha-amino terminus of substrates with the E2 Ube2w and facilitates the ubiquitination of lysine residues with the E2 UbcH5. While it is known that Ube2w directly interacts with disordered regions at the N-terminus of its substrates, it is unclear how CHIP and UbcH5 mediate substrate lysine selection. Here, we have decoupled the contributions of the E2, UbcH5, and the E3, CHIP, in ubiquitin transfer. We show that UbcH5 selects substrate lysine residues independent of CHIP, and CHIP participates in lysine selection by fine-tuning the subset of substrate lysines that are ubiquitinated. We also identify lysine 128 near the C-terminus of UbcH5 as a critical residue for efficient ubiquitin transfer by UbcH5 in both the presence and absence of CHIP. Together, these data demonstrate an important role for UbcH5/substrate interactions in mediating efficient ubiquitin transfer by the CHIP/UbcH5 complex.

[*]To whom correspondence should be addressed: K. Matthew Scaglione, PhD, Tel.: 919-660-8830; matt.scaglione@duke.edu.

Author contributions: A.K. and K.M.S. designed the overall study, wrote the manuscript, and performed the biochemical experiments. H.H performed and analyzed ubiquitination assays in Figures 2 and 3. V.V. and R.E.K. designed, performed, and analyzed the NMR-based experiments. T.K. and R.L.G. designed, performed, and analyzed the mass spectrometrybased experiments. All authors analyzed the results and reviewed and edited the manuscript.

Accession Codes (UniProtKB)
CHIP, Q9UNE7; UbcH5c, P61077; Ube2w, Q96B02; TAU, P10636; Hsp70, P0DMV8; Hsp90, P08238; ATXN3, P542252; Ubc13, P61088; Mms2, Q15619; Ube2k, P61086; Ube2e3, P51965

Conflict of Interest: The authors declare that they have no conflicts of interest with the contents of this article.

Keywords

ubiquitin; ubiquitin-conjugating enzyme; ubiquitin ligase; chaperone; protein degradation

INTRODUCTION

Ubiquitination of proteins regulates virtually every cellular process through the attachment of mono- or polyubiquitin chains to substrate proteins. Ubiquitination is accomplished by a cascade of three enzymes: E1 ubiquitin activating enzymes, E2 ubiquitin-conjugating enzymes, and E3 ubiquitin ligases. Typically, this results in the formation of an isopeptide bond between the C-terminus of ubiquitin and a lysine residue on the substrate. Structural data of some E2/E3 complexes strongly supports the role of E3 ubiquitin ligases in orientating substrate lysine residues in proximity to the active site of E2s (1–4); however, unlike these structures, CHIP exists in a dynamic tethered complex with its substrate adapter heat shock cognate 71 kDa protein (Hsc70) (5, 6). The dynamic nature of this complex has been proposed to allow CHIP the necessary flexibility to “search” for substrate residues on the wide range of client proteins that may be bound to Hsc70 (5). This raises the question of how CHIP functions with E2 ubiquitin conjugating enzymes to identify substrate residues.

In addition to the high degree of flexibility CHIP has with its substrate adapter Hsc70, it is also known that CHIP interacts with multiple E2s including Ube2w and UbcH5 (7). Interestingly, CHIP and Ube2w facilitate ubiquitination of the alpha-amino terminus of substrates while CHIP and UbcH5 ubiquitinate lysine residues (8, 9). This suggests that the E2 is participating in the selection of substrate residues with CHIP. This is supported by structural studies that show Ube2w facilitates N-terminal ubiquitination by directly binding disordered N-terminal regions of substrates with its C-terminus (10). While the mechanism Ube2w utilizes to select substrate residues is known, the role UbcH5 plays in facilitating lysine selection with CHIP is unclear. Here, we show that direct interactions between UbcH5 and substrate participate in lysine selection and demonstrate that these interactions are necessary for efficient ubiquitination. We further show that CHIP participates in lysine selection by preferentially stimulating ubiquitination of a subset of substrate lysine residues. Together, these data provide the first insight into how the CHIP/UbcH5 ubiquitination machinery selects substrate lysine residues.

MATERIALS AND METHODS

Constructs.

CHIP (Q9UNE7), ATXN3 (P54252), and Ube2w (Q96B02) were cloned into pGEX6p-1 as previously described (11). UbcH5c (P61077) in pET28a was obtained from Addgene (plasmid 12643). Ube1 (P22314), Tau (P10636), Hsp70 (Q9NZL4), and Hsp90 (P07900) were expressed using pET28a, pNG2, pMCSG7 and, pET151 vectors respectively. Mutations were introduced via QuikChange Lightning Mutagenesis Kit (Stratagene).

Protein Purification.

All proteins were expressed in Rosetta (DE3) cells. CHIP, ATXN3, and Ube2w were expressed as GST fusion proteins. For GST purification, cell pellets were lysed in NETN buffer (50mM Tris pH 7.5, 150mM NaCl, 0.5% NP-40, 0.2mM DTT, 1mM aprotinin, 1mM leupeptin, and 0.5mM PMSF), sonicated and clarified by centrifugation. Cell lysates were next tumbled with glutathione beads for 2 hours at 4°C, and glutathione beads were washed three times with NETN followed by three additional washes with kinase buffer (50mM Tris pH7.5, 50mM KCl, 0.2mM DTT). Following washing, glutathione beads were resuspended in 1:1 v:v ratio of kinase buffer and incubated with PreScission Protease (GE Healthcare) for 16 hours at 4°C. Finally, cleaved protein was pooled, concentrated, and gel filtered using an Enrich SEC 70 column (Biorad). Hsp70 and Hsp90 contain a 6xHis tag and were purified by nickel chromatography. Cell pellets expressing Hsp70 or Hsp90 were lysed in buffer A (50mM Tris pH7.5, 150mM NaCl, 0.5% Triton X-100, 0.2mM DTT, 1mM aprotinin, 1mM leupeptin, and 0.5mM PMSF), were sonicated, and then centrifuged. Cell lysates were tumbled with NiNTA (Qiagen) for 1 hour at 4°C. Ni-NTA was washed three times with buffer A, three times with buffer B (50mM Tris pH7.5, 500mM NaCl, and 0.2mM DTT), and three times with buffer C (50mM Tris pH7.5, 150mM NaCl, 20mM Imidazole, and 0.2mM DTT). Protein was eluted in buffer C with an additional 280mM Imidazole. Purified protein was pooled, concentrated, and gel filtered using an Enrich SEC 650 column (Biorad) in kinase buffer. Pure fractions were combined and concentrated. For E1, UbcH5, and tau recombinant protein was purified as previously described (12–14).

Ubiquitination Assays.

Reactions were performed as previously established (15). For CHIP dependent ubiquitination assays we used 1μM of CHIP and 1μM of E2, 1μM substrate, and $E1^{mix}$. $E1^{mix}$ consists of 100nM E1, 250μM Ub, 2.5mM ATP, and 2.5mM $MgCl_2$. All reactions were performed in kinase buffer. For E3 independent ubiquitination reactions, 5μM of E2, 20μM of substrate, and $E1^{mix}$ was used with reactions carried out for four hours in kinase buffer. All reactions were performed at 37°C. Reactions were stopped by addition of Laemmli buffer and boiling, followed by separation of proteins by SDS-PAGE and visualization by immunoblotting with the appropriate antibodies.

Kinetic characterization of ubiquitin transfer.

Ubiquitination reactions were performed with increasing concentrations of JD with 5μM UbcH5 in the absence of an E3 and visualized by Coomassie stain. Ubiquitination reactions performed with greater than 40μM of JD were diluted to 40μM prior to loading 10μL from each ubiquitination reaction for visualization by Coomassie stain and relative quantification was performed by comparison to monoubiquitinated JD standards. Ubiquitinated JD was quantitated using Image-J, plotted using GraphPad Prism software and fitted to Michaelis-Menten kinetics.

NMR Spectroscopy.

All NMR samples were prepared in 25mM sodium phosphate (pH 7.0) and 150mM NaCl using either 90% H2O/D2O or 100% D2O. Samples for UbcH5 utilized uniformly 15-

Nlabeled protein. Titration experiments involving 15N – UbcH5 were performed by addition of unlabeled Hsp70. The magnitude of chemical shift perturbations for each resonance was quantified in Hz according to the equation Δδj=((Δδj15N)2 + (Δδj 1H)2)1/2. Data collection for resonance assignments utilized standard three-dimensional NMR techniques collected on INOVA 600 and 800 MHz spectrometers (Varian) at Pacific Northwest National Labs (PNNL). All spectra were collected at 25°C. Data were processed using NMR-Pipe/ NMRDRaw (16) and visualized with NMRView (17).

Relative Quantification of Substrate Lysine Ubiquitination using TMT-labeling.

Ubiquitination reactions were performed in the presence or absence of E3, dialyzed into 50mM HEPES, pH 8.0, concentrated to 2 mg/mL, and centrifuged at 16,000 x *g* at 4°C for 10 minutes. 100μg of each ubiquitination reaction was brought to a final volume of 100μL with 100mM TEAB (triethyl ammonium bicarbonate) containing 10mM TCEP (tris(2-carboxyethyl)phosphine). Samples were incubated at 55°C for one hour followed by subsequent addition of 18mM iodoacetamide for one hour at room temperature and acetone precipitation. Samples were then centrifuged at 8000 x *g* for 10 minutes at 4°C and acetone was removed. Samples were resuspended in 100μL of 50mM TEAB. 2.5μL of trypsin was added to each sample for digestion overnight at 37°C. TMT labeling was performed using TMTsixplex™ Isobaric Label Reagent Set per manufacturer's instructions (Thermo Scientific). In brief, digested peptides were TMT labeled by adding 100μg of trypsin-digested peptide sample to 0.8mg of each TMT isobaric label that had been previously dissolved in 41μL of anhydrous acetonitrile. Labeling was allowed to proceed for one hour at room temperature at which time the reaction was quenched by addition of 8μL of 5% hydroxylamine to each sample for 15 min. Experimental triplicates with differing TMT mass tags were combined in triplicate, desalted with C18 microspin columns, and dried under vacuum.

Mass Spectrometry.

Lyophilized peptide sample was reconstituted in mobile phase A (5% acetonitrile, 0.1% (v/v) formic acid in water) to a final concentration of 600 ng/μL. Samples were analyzed by liquid chromatography tandem mass spectrometry using a NanoLC Ultra 2D HPLC (Eksigent, Dublin, CA) in line with a Q Exactive Hybrid Quadrupole Orbitrap mass spectrometer (Thermo, Waltham, MA). Samples were analyzed in triplicate for both data-dependent acquisition (DDA) and parallel reaction monitoring (PRM) analyses. For each sample injection, 1μl sample was loaded onto a hand-packed trap (75μm ID, 3cm, ProntoSIL C_{18} AQ, 3μm, 200Å (Bischoff Chromatography, Leonberg, Germany)), and washed with mobile phase A for 10 min at 2 μl/min before elution onto a PicoChip column (75μm ID, 10.5cm, Reprosil-PUR C_{18}-AQ, 3μm, 120Å (New Objective, Woburn, MA)). Peptides were separated using a linear gradient from 0% to 25.0% B in 80 minutes at a flow rate of 300 nL/min where mobile phase B was 95% acetonitrile, 0.1% (v/v) formic acid in water.

For DDA, MS1 spectra were acquired using a target setting of 3E6 ions, an accumulation time of 120ms, and scanned at a resolution of 140,000 (at 200 *m/z*) over a scan range of 350 – 1800 *m/z*. Each MS1 scan was followed by HCD fragmentation of the 15 most abundant precursor ions with a charge state between +2 and +7 and MS2 spectra were scanned at a

resolution of 35,000 (at 200 *m/z*). Data were analyzed in Proteome Discoverer 2.1 (Thermo) using Sequest HT and MS Amanda search algorithms, Percolator (18) for post-search validation, and ptmRS (19) to aid in modification site localization. Data were searched against human SwissProt database (03/2016, 42,091 sequences) and an appropriately modified CHIP ligase sequence. The search included semi-tryptic digestion and two missed cleavages to account for the modification of lysine residues interfering with cleavage sites. Static modifications included the TMT label (+229.163 Da) at any N-terminus and cysteine carbamidomethylation. Dynamic modifications included oxidation at methionine, TMT label modification at lysine residues, and the GlyGly-TMT label modification (+343.206 Da) representing ubiquitinated lysines. Precursor mass tolerance was set to 10 ppm, fragment mass tolerance to 0.02 Da, and isolation interference to 30%. Peptides identified with a localized GlyGly-TMT modification were selected for subsequent PRM analyses.

For PRM, an isolation list containing the monoisotopic *m/z,* charge state, and retention time schedule (measured retention time ± 5.0 minutes) of GlyGly-TMT modified peptides determined from the DDA analyses were exported from Proteome Discoverer. This list contained 26 ions for Hsp70 ±CHIP. Selected precursors were fragmented and MS^2 spectra were collected as above with an isolation window of 0.8 *m/z*. PRM data were analyzed using the same workflow as above, and results were imported into Skyline (20) for quantitative analyses. MS2 fragment ion abundances were visualized chromatographically and multiple MS2 scans derived from the same precursor were integrated over time. The use of multiple scans for TMT-based quantitation benefits quantitative accuracy of the measured ratios for ubiquitination of Hsp70 in the presence or absence of CHIP ligase. The ratios of ubiquitination in the presence and absence of CHIP ligase were visualized using Protter (21) and are shown in figure [7a] for Hsp70.

RESULTS

Establishment of an E3 independent ubiquitination assay.

CHIP can stimulate ubiquitination of either the alpha amino-terminus or internal lysine residues of the same substrate depending on whether Ube2w or UbcH5 is recruited (8). This suggests that either E2s participate in selecting the residues ubiquitin is attached to or that the active site of Ube2w and UbcH5 are orientated differently when bound to CHIP. To test the later hypothesis, we generated structural overlays of UbcH5 and Ube2w bound to CHIP and these predict there is no difference in the position of the E2 active site cysteine (Fig 1a). This, along with published data, suggests that inherent properties of the E2 contribute to substrate residue selection (10).

We next wanted to establish an assay to decouple the activity of E2s and E3s. Previously, E2s including Rad6 and Ube2w have been shown to ubiquitinate substrates in the absence of an E3 ligase (10, 22). To establish a similar assay with CHIP substrates we used elevated concentrations of E2 and substrate in the absence of CHIP and found that ubiquitination of the Josephin domain (JD) of ataxin-3 (ATXN3), a CHIP substrate (7, 8, 23–26), could occur in the absence of an E3 (Fig 1b and c). To determine if this was generalizable to other substrates, we repeated E3 independent ubiquitination assays using a variety of CHIP substrates, including heat shock protein 70 (Hsp70), heat shock protein 90 (Hsp90) and tau.

In each case we observed ubiquitination of substrates in the absence of CHIP (Fig 1d-f). Together, these data establish an assay that decouples E2 and E3 function allowing for independent assessment of the role of each enzyme in ubiquitin transfer.

Ube2w and UbcH5 maintain substrate residue specificity in the absence of CHIP.

Previous work demonstrated that the CHIP/Ube2w pair ubiquitinates the alpha- amino terminus of ATXN3 and lysine-less ATXN3 (^{KO}ATXN-3) and blocking ATXN3's N-terminus with GST (^{GST}ATXN3) prevented CHIP/Ube2w mediated ubiquitination (8). Alternatively, the CHIP/UbcH5 pair ubiquitinated ATXN3 and ^{GST}ATXN3 but failed to ubiquitinate ^{KO}ATXN3, consistent with ubiquitination of substrate lysine residues (8). To confirm that in the absence of CHIP, Ube2w ubiquitinates the alpha-amino terminus of substrates and UbcH5 selectively ubiquitinates lysine residues we performed E3 independent ubiquitination assays utilizing ATXN3, ^{KO}ATXN3, or ^{GST}ATXN3 as the substrate. Consistent with UbcH5 and Ube2w dictating substrate residue specificity, UbcH5 ubiquitinated ^{GST}ATXN3, but not ^{KO}ATXN3 (Figure 2a) and Ube2w ubiquitinated ^{KO}ATXN3, but not ^{GST}ATXN3 in the absence of CHIP (Figure 2b). Together this data is consistent with UbcH5 and Ube2w maintaining substrate residue selectivity in the absence of an E3.

In addition to determining that E2s retain their ability to select substrate residues in the absence of CHIP, we also wanted to confirm that the ubiquitination of substrates was selective between different substrates and E2s. To accomplish this, we performed E3 independent ubiquitination assays to determine if other E2s could ubiquitinate the JD of ATXN3 in the absence of CHIP. We observed that UbcH5, but not Ubc13/Mms2, Ube2k, or Ube2e3 ubiquitinated the JD in the absence of CHIP (Figure 3). Importantly, all E2s were active as we observed the formation of polyubiquitin chains by Ubc13/Mms2, di-ubiquitin by Ube2k, and autoubiquitination by Ube2e3 (Figure 3).

CHIP stimulates ubiquitination via two distinct mechanisms.

In cells, E3s are important for facilitating transfer of ubiquitin onto substrates. CHIP, like other RING/U-box type E3s, is expected to stimulate the transfer of ubiquitin from E2 to substrate through two mechanisms: binding to CHIP's U-box promotes a closed E2~Ub conformation that has increased reactivity with substrate lysines (27, 28), and CHIP serves as a scaffold to bring the E2~Ub and substrate into close proximity (29). We next wanted to confirm that the presence of CHIP, or CHIP's U-box domain, stimulated ubiquitin transfer by E2s. To accomplish this, we performed ubiquitination assays either without CHIP, with CHIP's U-box domain, or with full-length CHIP (Fig. 4). Consistent with the U-box activating E2~Ub conjugates, the addition of CHIP's U-box domain stimulated ubiquitin transfer (Figs. 4a and b). Moreover, full-length CHIP led to a robust increase in ubiquitination consistent with a role for CHIP's scaffolding function (Fig 4a and b). Together, these data are consistent with a bifunctional role for CHIP in stimulating ubiquitin transfer.

To further characterize our E3 independent ubiquitination assay, we performed reactions with increasing amounts of substrate to determine K_M and k_{cat}. For these assays, we used a

construct of JD engineered to contain a single, physiologically important lysine residue at position 117 (JD^{K117}) (26), and lysine-less ubiquitin to limit ubiquitin transfer to a single monoubiquitination event. Employing this assay, we found that ubiquitin transfer was extremely inefficient in the absence of CHIP, occurring at a rate of approximately one ubiquitin per minute to JD^{K117} (Fig 5a and b, table 1). We next wanted to determine how interaction with CHIP altered ubiquitin transfer to JD^{K117} by UbcH5. Because CHIP stimulates ubiquitin transfer by two distinct mechanisms, activating UbcH5 and bringing UbcH5 and substrate into close proximity, we set out to assess each contribution independently. We first determined the amount of CHIP's U-box domain necessary to maximally activate UbcH5 (Fig 5c) and used a saturating amount of U-box in subsequent ubiquitination assays. As expected, the presence of U-box did not alter the K_M but led to a ~20-fold increase in k_{cat} (Fig 5d and e, Table 1). We were unable to determine how the scaffolding effect of CHIP altered K_M and k_{cat} due to the confounding effect of autoubiquitination in our assays (data not shown). Together these data support a bipartite role for CHIP in stimulating transfer of ubiquitin from UbcH5 to substrate.

Defining the role of the E2 UbcH5 and the E3 CHIP in lysine selection.

Substrate ubiquitination by UbcH5 in the absence of an E3 suggests that interactions between substrate and the E2~Ub conjugate alone may be sufficient for determining substrate lysine preference. The JD of ATXN3 contains six surface exposed lysine residues that are accessible for ubiquitination (Fig 6a). To determine if any of these lysine residues become preferentially ubiquitinated, ubiquitination assays were performed using JD constructs containing a single surface exposed lysine residue, with remaining lysine residues mutated to arginine. When ubiquitination assays were performed with these constructs the JD construct containing only K117 was preferentially ubiquitinated (26). To determine if the preferential ubiquitination of JD occurs at K117 when all lysine residues of the JD are present, we performed ubiquitination assays in the presence of JD or with a construct of the JD where K117 was mutated to arginine (JD^{K117R}). In the presence of CHIP, ubiquitination of JD^{K117R} was markedly decreased confirming that K117 is preferentially ubiquitinated (Fig 6b). To determine if preferential ubiquitination of K117 is directed by UbcH5 or by CHIP, we performed E3 independent ubiquitination assays with JD or JD^{K117R} and found that ubiquitination of JD^{K117R} was severely inhibited, consistent with a role for UbcH5 in lysine selection (Fig 6c). Together, these data suggest that UbcH5 can identify K117 of the JD in the absence of CHIP.

While the CHIP/UbcH5 pair monoubiquitinates ATXN3 at a single lysine residue, CHIP is known to polyubiquitinate many substrates on multiple lysine residues. We next wanted to assess the influence of CHIP in defining substrate lysine selection with UbcH5 on substrates that are ubiquitinated on multiple lysine residues. To accomplish this, we performed mass spectrometry and quantified the ratio of lysine modification on Hsp70, a bona-fide CHIP substrate (30), in the presence and absence of CHIP. Importantly, we observed ubiquitination of the same lysine residues in the presence and absence of CHIP, with CHIP stimulating ubiquitination of only a small subset of lysine residues in the lid domain of Hsp70 (Fig 7a and b). Interestingly, this region of Hsp70 is in proximity to Hsp70's substrate binding site, consistent with a role for CHIP in positioning Hsp70-bound misfolded protein in close

proximity to the E2~Ub conjugate. This suggests that while UbcH5 has the ability to recognize substrate lysine residues in the absence of CHIP, CHIP participates in lysine selection and stimulates ubiquitination of only a subset of lysines.

Identification of UbcH5 residues important for mediating substrate binding.

Our data indicate that UbcH5 can identify substrate lysines in the absence of an E3, suggesting that direct interactions between UbcH5 and substrate occur. To determine the residues on UbcH5 that interact with substrate, we performed NMR titrations with ^{15}N-labelled UbcH5 and one of its substrates, Hsp70. Upon titration of Hsp70, a subset of ^{15}N-UbcH5 resonances were broadened (Fig 8a-c). Among the broadened resonances, K128 was notable because this residue is in contact with the nucleosome core particle substrate in the crystal structure of the Polycomb repressive complex 1 (PRC1) ubiquitination module (3). In this complex, mutation of K128 disrupts interactions with the nucleosome core particle but has no effect on UbcH5's catalytic activity (3). To determine if K128 of UbcH5c plays a substrate-contacting role in the CHIP/UbcH5c/Hsp70 complex, we titrated Hsp70 with ^{15}N-labelled UbcH5 mutant, peak broadening UbcH5^{K128E}. The observed peak broadening was greatly decreased upon titration of Hsp70 with ^{15}N-labelled UbcH5c^{K128E}, consistent with the E2 mutant having a lower affinity for Hsp70 (Fig 8c).

To confirm that K128 of UbcH5 has a functional role in transfer of ubiquitin by the CHIP/UbcH5 pair, we performed ubiquitination assays with CHIP and either wild-type UbcH5 or UbcH5c^{K128E}. Indeed, the UbcH5c^{K128E} mutant had a dramatically decreased ability to ubiquitinate multiple substrates including ATXN3, Hsp70, and Hsp90 (Fig 8d–f). In addition to decreased activity with CHIP, the UbcH5^{K128E} mutant also had decreased activity in the absence of CHIP consistent with a role for K128 in mediating UbcH5/substrate interactions (Fig 8g–i). Together, these data suggest an important role for UbcH5/substrate interactions in ubiquitin transfer.

DISCUSSION

Our work stems from the observation that when paired with different E2s CHIP ubiquitinates different residues on the same substrate (8). While it is well established that Ube2w can bind disordered N-termini of its substrates, it was unclear how CHIP and UbcH5 identified substrate lysines. While some E2/E3 complexes orientate substrate residues next to the active site of the E2 (1–4), it is unclear how CHIP would position substrate lysine near the active site of UbcH5 for several reasons. First, CHIP exists in a dynamic tethered complex with Hsc70 where the only major contacts between CHIP and Hsc70 occur between the C-terminal IEEVD motif of Hsc70 and tetracopeptide repeat (TPR) domain of CHIP (5). Second, CHIP ubiquitinates chaperone bound client proteins. This is important because chaperones interact with a large number of substrates, potentially binding multiple sites within the same substrate. For example, the Hsp70 homolog DnaK is expected to bind to 98% of the *Escherichia coli* (*E.coli*) proteome with an estimated average of 23 binding sites per protein (31). On a proteome wide scale this would result in over 95,000 potential DnaK binding sites (31). Extrapolated to the human genome which encodes roughly five times as many protein coding genes, this would suggest that chaperones have ~500,000

binding sites and thus ~500,000 potential presentations of misfolded proteins for CHIP to ubiquitinate. This suggests that the dynamic nature of the CHIP/Hsc70 complex provides a required mechanism for accommodating a large array of potential substrates.

While we observed that interactions between UbcH5 and substrate are important for ubiquitin transfer and lysine selection, there is an abundance of evidence for the role of ubiquitin ligases in positioning substrate lysines near the E2 (1–4). Here, we show that while the same subset of lysines are ubiquitinated in the presence and absence of CHIP, CHIP stimulates the ubiquitination of only a subset of lysines (Fig 7). This suggests that CHIP binds and orientates the substrate in a manner that preferentially presents certain regions of the substrate in close proximity to UbcH5, which can then bind and ubiquitinate the substrate. While our kinetic data suggest a low affinity interaction between UbcH5 and substrate (Fig 4), the scaffolding effect of CHIP increases the local concentration of E2 and substrate to a point where even low affinity interactions would become physiologically relevant. Overall, our findings are consistent with structures of E3s that reveal positioning of substrate lysine residues in close proximity with E2s (1–4).

The role of E2s in facilitating substrate residue selection is an emerging trend in ubiquitination, however the role of substrate/UbcH5 interactions and identification of individual contributions of E2 and E3 in substrate ubiquitination remain largely unexplored. In addition to our data showing a direct interaction between UbcH5 and substrate, the structure of the PRC1 ubiquitination module implies that interactions between UbcH5 and nucleosomal DNA are important for the efficient ubiquitination of K119 of histone H2A (3). In both our studies and studies investigating interactions between UbcH5 and the PRC1 ubiquitination module, interactions between K128 of UbcH5 and substrate were detected (Fig 8). In the case of the nucleosome core particle, UbcH5-K128 contacts nucleosomal DNA, while we find that K128 of UbcH5 facilitates interactions between Hsp70 and UbcH5. This suggests that interacting partners, including proteins, DNA, and potentially other molecules can directly influence substrate ubiquitination by binding E2s. In the future, it will be interesting to see if other types of molecules interact with E2s to stimulate efficient substrate ubiquitination.

In addition to interactions with the substrates being ubiquitinated, many E2s that extend polyubiquitin chains directly interact with the substrate acceptor ubiquitin. For example, Ube2S utilizes its C-terminus to interact with acceptor ubiquitin molecules during the formation of K11-linked polyubiquitin chains (32), whereas Mms2 orientates K63 of ubiquitin next to the active site of Ubc13 in the Ubc13/Mms2 heterodimer (33, 34), and the E2s Ube2k and Ube2g2 interact with both donor and acceptor ubiquitin molecules to facilitate K48-linked chains (35, 36). UbcH5's backside has also been implicated in the extension of polyubiquitin chains; in this case S22 of UbcH5 interacts with the acceptor ubiquitin to promote polyubiquitin chain formation (14). Moving forward, it will be important to further define the extent that UbcH5 contributes to substrate ubiquitination when paired with additional E3 ligases. Additionally it will be important to determine regions of other E2s that interact with substrate to determine if E2 participation in lysine selection is a recurring theme among other E2/E3 pairs.

CONCLUSION

Here, we have identified a key interaction between the E2 UbcH5 and substrate that is necessary for efficient ubiquitination by the UbcH5/CHIP pair. To differentiate the contribution of E2 and E3 to the mechanism of lysine selection during ubiquitin transfer, we established an assay that decouples E2 and E3 function (Fig 1–5). Using this assay, we demonstrated that UbcH5 ubiquitinates the same subset of substrate lysines in the presence or absence of CHIP (Figure 6–7). We also observed that CHIP participates in selecting substrate lysine residues by stimulating ubiquitination of only a subset of lysine residues modified by UbcH5 (Fig 7). We further showed that substrates directly interact with UbcH5 and that this interaction is necessary for efficient substrate ubiquitination (Fig 8). Together, these results suggest critical roles for both UbcH5 and CHIP in substrate lysine selection.

Acknowledgments:

We thank members of the Scaglione lab for helpful comments and critiques of the manuscript. This work was supported in whole or in part by National Institute of Health Grants R00 NS073936 and R35GM119544 to KMS, and R01 GM088055 to REK. This work was also supported in part by a grant from the National Niemann-Pick Disease Foundation to AK.

REFERENCES

1. Brown NG, VanderLinden R, Watson ER, Weissmann F, Ordureau A, Wu KP, Zhang W, Yu S, Mercredi PY, Harrison JS, Davidson IF, Qiao R, Lu Y, Dube P, Brunner MR, Grace CR, Miller DJ, Haselbach D, Jarvis MA, Yamaguchi M, Yanishevski D, Petzold G, Sidhu SS, Kuhlman B, Kirschner MW, Harper JW, Peters JM, Stark H, Schulman BA. Dual RING E3 Architectures Regulate Multiubiquitination and Ubiquitin Chain Elongation by APC/C. Cell. 2016;165(6):1440–53. doi: 10.1016/j.cell.2016.05.037.. [PubMed: 27259151]
2. Chang L, Zhang Z, Yang J, McLaughlin SH, Barford D. Atomic structure of the APC/C and its mechanism of protein ubiquitination. Nature. 2015;522(7557):450–4. doi: 10.1038/nature14471. [PubMed: 26083744]
3. McGinty RK, Henrici RC, Tan S. Crystal structure of the PRC1 ubiquitylation module bound to the nucleosome. Nature. 2014;514(7524):591–6. doi: 10.1038/nature13890. [PubMed: 25355358]
4. Streich FC, Jr., Lima CD. Capturing a substrate in an activated RING E3/E2-SUMO complex. Nature. 2016;536(7616):304–8. doi: 10.1038/nature19071. [PubMed: 27509863]
5. Smith MC, Scaglione KM, Assimon VA, Patury S, Thompson AD, Dickey CA, Southworth DR, Paulson HL, Gestwicki JE, Zuiderweg ER. The E3 ubiquitin ligase CHIP and the molecular chaperone Hsc70 form a dynamic, tethered complex. Biochemistry. 2013;52(32):5354–64. Epub 2013/07/20. doi: 10.1021/bi4009209. [PubMed: 23865999]
6. Quintana-Gallardo L, Martin-Benito J, Marcilla M, Espadas G, Sabido E, Valpuesta JM. The cochaperone CHIP marks Hsp70- and Hsp90-bound substrates for degradation through a very flexible mechanism. Sci Rep. 2019;9(1):5102 Epub 2019/03/27. doi: 10.1038/s41598-019-41060-0. [PubMed: 30911017]
7. Scaglione KM, Zavodszky E, Todi SV, Patury S, Xu P, Rodriguez-Lebron E, Fischer S, Konen J, Djarmati A, Peng J, Gestwicki JE, Paulson HL. Ube2w and ataxin-3 coordinately regulate the ubiquitin ligase CHIP. Mol Cell. 2011;43(4):599–612. doi: 10.1016/j.molcel.2011.05.036. [PubMed: 21855799]
8. Scaglione KM, Basrur V, Ashraf NS, Konen JR, Elenitoba-Johnson KS, Todi SV, Paulson HL. The ubiquitin-conjugating enzyme (E2) Ube2w ubiquitinates the N terminus of substrates. J Biol Chem. 2013;288(26):18784–8. doi: 10.1074/jbc.C113.477596. [PubMed: 23696636]
9. Tatham MH, Plechanovova A, Jaffray EG, Salmen H, Hay RT. Ube2W conjugates ubiquitin to alpha-amino groups of protein N-termini. Biochem J. 2013;453(1):137–45. doi: 10.1042/BJ20130244. [PubMed: 23560854]

10. Vittal V, Shi L, Wenzel DM, Scaglione KM, Duncan ED, Basrur V, Elenitoba-Johnson KS, Baker D, Paulson HL, Brzovic PS, Klevit RE. Intrinsic disorder drives N-terminal ubiquitination by Ube2w. Nat Chem Biol. 2015;11(1):83–9. doi: 10.1038/nchembio.1700. [PubMed: 25436519]
11. Winborn BJ, Travis SM, Todi SV, Scaglione KM, Xu P, Williams AJ, Cohen RE, Peng J, Paulson HL. The deubiquitinating enzyme ataxin-3, a polyglutamine disease protein, edits Lys63 linkages in mixed linkage ubiquitin chains. J Biol Chem. 2008;283(39):26436–43. doi: 10.1074/jbc.M803692200. [PubMed: 18599482]
12. Barghorn S, Biernat J, Mandelkow E. Purification of recombinant tau protein and preparation of Alzheimer-paired helical filaments in vitro. Methods Mol Biol. 2005;299:35–51. Epub 2005/06/28. doi: 10.1385/1-59259-874-9:035. [PubMed: 15980594]
13. Berndsen CE, Wolberger C. A spectrophotometric assay for conjugation of ubiquitin and ubiquitin-like proteins. Anal Biochem. 2011;418(1):102–10. Epub 2011/07/21. doi: 10.1016/j.ab.2011.06.034. [PubMed: 21771579]
14. Brzovic PS, Lissounov A, Christensen DE, Hoyt DW, Klevit RE. A UbcH5/ubiquitin noncovalent complex is required for processive BRCA1-directed ubiquitination. Mol Cell. 2006;21(6):873–80. doi: 10.1016/j.molcel.2006.02.008. [PubMed: 16543155]
15. Kanack AJ, Newsom OJ, Scaglione KM. Most mutations that cause spinocerebellar ataxia autosomal recessive type 16 (SCAR16) destabilize the protein quality-control E3 ligase CHIP. J Biol Chem. 2018;293(8):2735–43. Epub 2018/01/11. doi: 10.1074/jbc.RA117.000477. [PubMed: 29317501]
16. Delaglio F, Grzesiek S, Vuister GW, Zhu G, Pfeifer J, Bax A. NMRPipe: a multidimensional spectral processing system based on UNIX pipes. J Biomol NMR. 1995;6(3):277–93. [PubMed: 8520220]
17. Johnson BA, Blevins RA. NMR View: A computer program for the visualization and analysis of NMR data. J Biomol NMR. 1994;4(5):603–14. doi: 10.1007/BF00404272. [PubMed: 22911360]
18. Kall L, Canterbury JD, Weston J, Noble WS, MacCoss MJ. Semi-supervised learning for peptide identification from shotgun proteomics datasets. Nat Methods. 2007;4(11):923–5. doi: 10.1038/nmeth1113. [PubMed: 17952086]
19. Taus T, Kocher T, Pichler P, Paschke C, Schmidt A, Henrich C, Mechtler K. Universal and confident phosphorylation site localization using phosphoRS. J Proteome Res. 2011;10(12):5354–62. doi: 10.1021/pr200611n. [PubMed: 22073976]
20. MacLean B, Tomazela DM, Shulman N, Chambers M, Finney GL, Frewen B, Kern R, Tabb DL, Liebler DC, MacCoss MJ. Skyline: an open source document editor for creating and analyzing targeted proteomics experiments. Bioinformatics. 2010;26(7):966–8. doi: 10.1093/bioinformatics/btq054. [PubMed: 20147306]
21. Omasits U, Ahrens CH, Muller S, Wollscheid B. Protter: interactive protein feature visualization and integration with experimental proteomic data. Bioinformatics. 2014;30(6):884–6. doi: 10.1093/bioinformatics/btt607. [PubMed: 24162465]
22. Jentsch S, McGrath JP, Varshavsky A. The yeast DNA repair gene RAD6 encodes a ubiquitinconjugating enzyme. Nature. 1987;329(6135):131–4. doi: 10.1038/329131a0. [PubMed: 3306404]
23. Williams AJ, Knutson TM, Colomer Gould VF, Paulson HL. In vivo suppression of polyglutamine neurotoxicity by C-terminus of Hsp70-interacting protein (CHIP) supports an aggregation model of pathogenesis. Neurobiol Dis. 2009;33(3):342–53. doi: 10.1016/j.nbd.2008.10.016. [PubMed: 19084066]
24. Tsou WL, Burr AA, Ouyang M, Blount JR, Scaglione KM, Todi SV. Ubiquitination regulates the neuroprotective function of the deubiquitinase ataxin-3 in vivo. J Biol Chem. 2013;288(48):34460–9. doi: 10.1074/jbc.M113.513903. [PubMed: 24106274]
25. Faggiano S, Menon RP, Kelly GP, Todi SV, Scaglione KM, Konarev PV, Svergun DI, Paulson HL, Pastore A. Allosteric regulation of deubiquitylase activity through ubiquitination. Front Mol Biosci. 2015;2:2 Epub 2015/05/20. doi: 10.3389/fmolb.2015.00002. [PubMed: 25988170]
26. Todi SV, Scaglione KM, Blount JR, Basrur V, Conlon KP, Pastore A, Elenitoba-Johnson K, Paulson HL. Activity and cellular functions of the deubiquitinating enzyme and polyglutamine

disease protein ataxin-3 are regulated by ubiquitination at lysine 117. J Biol Chem. 2010;285(50):39303–13. doi: 10.1074/jbc.M110.181610. [PubMed: 20943656]

27. Pruneda JN, Littlefield PJ, Soss SE, Nordquist KA, Chazin WJ, Brzovic PS, Klevit RE. Structure of an E3:E2~Ub complex reveals an allosteric mechanism shared among RING/U-box ligases. Mol Cell. 2012;47(6):933–42. doi: 10.1016/j.molcel.2012.07.001. [PubMed: 22885007]
28. Plechanovova A, Jaffray EG, Tatham MH, Naismith JH, Hay RT. Structure of a RING E3 ligase and ubiquitin-loaded E2 primed for catalysis. Nature. 2012;489(7414):115–20. doi: 10.1038/nature11376. [PubMed: 22842904]
29. Metzger MB, Pruneda JN, Klevit RE, Weissman AM. RING-type E3 ligases: master manipulators of E2 ubiquitin-conjugating enzymes and ubiquitination. Biochim Biophys Acta. 2014;1843(1):47–60. doi: 10.1016/j.bbamcr.2013.05.026. [PubMed: 23747565]
30. Qian SB, McDonough H, Boellmann F, Cyr DM, Patterson C. CHIP-mediated stress recovery by sequential ubiquitination of substrates and Hsp70. Nature. 2006;440(7083):551–5. Epub 2006/03/24. doi: 10.1038/nature04600. [PubMed: 16554822]
31. Srinivasan SR, Gillies AT, Chang L, Thompson AD, Gestwicki JE. Molecular chaperones DnaK and DnaJ share predicted binding sites on most proteins in the E. coli proteome. Mol Biosyst. 2012;8(9):2323–33. doi: 10.1039/c2mb25145k. [PubMed: 22732719]
32. Wickliffe KE, Lorenz S, Wemmer DE, Kuriyan J, Rape M. The mechanism of linkage-specific ubiquitin chain elongation by a single-subunit E2. Cell. 2011;144(5):769–81. doi: 10.1016/j.cell.2011.01.035. [PubMed: 21376237]
33. Eddins MJ, Carlile CM, Gomez KM, Pickart CM, Wolberger C. Mms2-Ubc13 covalently bound to ubiquitin reveals the structural basis of linkage-specific polyubiquitin chain formation. Nat Struct Mol Biol. 2006;13(10):915–20. doi: 10.1038/nsmb1148. [PubMed: 16980971]
34. VanDemark AP, Hofmann RM, Tsui C, Pickart CM, Wolberger C. Molecular insights into polyubiquitin chain assembly: crystal structure of the Mms2/Ubc13 heterodimer. Cell. 2001;105(6):711–20. [PubMed: 11440714]
35. Middleton AJ, Day CL. The molecular basis of lysine 48 ubiquitin chain synthesis by Ube2K. Sci Rep. 2015;5:16793. doi: 10.1038/srep16793. [PubMed: 26592444]
36. Liu W, Shang Y, Zeng Y, Liu C, Li Y, Zhai L, Wang P, Lou J, Xu P, Ye Y, Li W. Dimeric Ube2g2 simultaneously engages donor and acceptor ubiquitins to form Lys48-linked ubiquitin chains. EMBO J. 2014;33(1):46–61. doi: 10.1002/embj.201385315. [PubMed: 24366945]

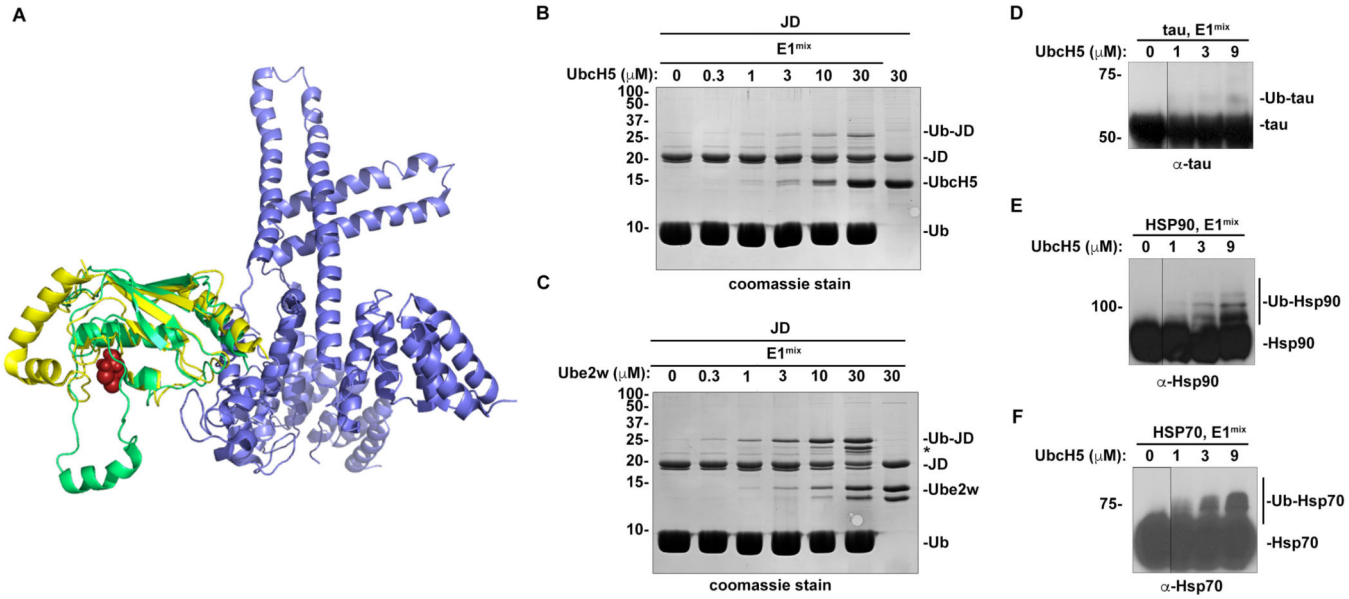

Figure 1. Establishment of an E3-independent ubiquitination assay.

A, Ube2w and UbcH5's active site cysteine residues are in the same location when bound to CHIP. CHIP (blue, PDB ID: 2C2L) was aligned with UbcH5 bound to CHIP's U-box domain (yellow, PDB ID: 2OXQ). The solution structure of Ube2w (green, PDB ID: 2MT6) was then aligned to UbcH5. E2 active site cysteines are shown in red. *B,* Elevated concentrations of E2 and substrate bypass the need for an E3 in *in vitro* ubiquitination assays. Ubiquitination assays using 20μM JD were performed with the indicated concentrations of the E2 UbcH5c. Reactions were visualized by Coomassie stain. *C,* Same as (B) with Ube2w as the E2. Asterisk indicates autoubiquitinated Ube2w. *D,* tau ubiquitination assays were performed with increasing concentrations of UbcH5 in the absence of E3 and analyzed by immunoblotting. *E,* Same as (D) with Hsp90 as the substrate. *F,* Same as (D) with Hsp70 as the substrate.

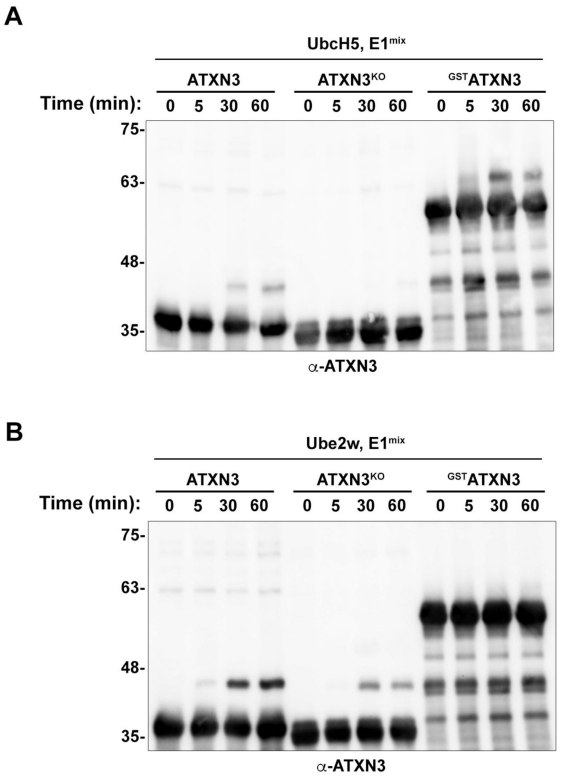

Figure 2: Ube2w and UbcH5 retain substrate residue selectively in the absence of CHIP.

(A) UbcH5 ubiquitinates lysine residues in the absence of CHIP. E3 independent ubiquitination assays were performed with UbcH5 and either ATXN3, ATXN3^{KO}, or ^{GST}ATXN3 as the substrate. Samples were visualized by Western blot analysis. (B) Ube2w ubiquitinates the N-termini, but not internal lysine residues in the absence of an E3. E3 independent ubiquitination assays were performed with Ube2w and either ATXN3, ATXN3^{KO}, or ^{GST}ATXN3 as the substrate. Samples were visualized by Western blot analysis.

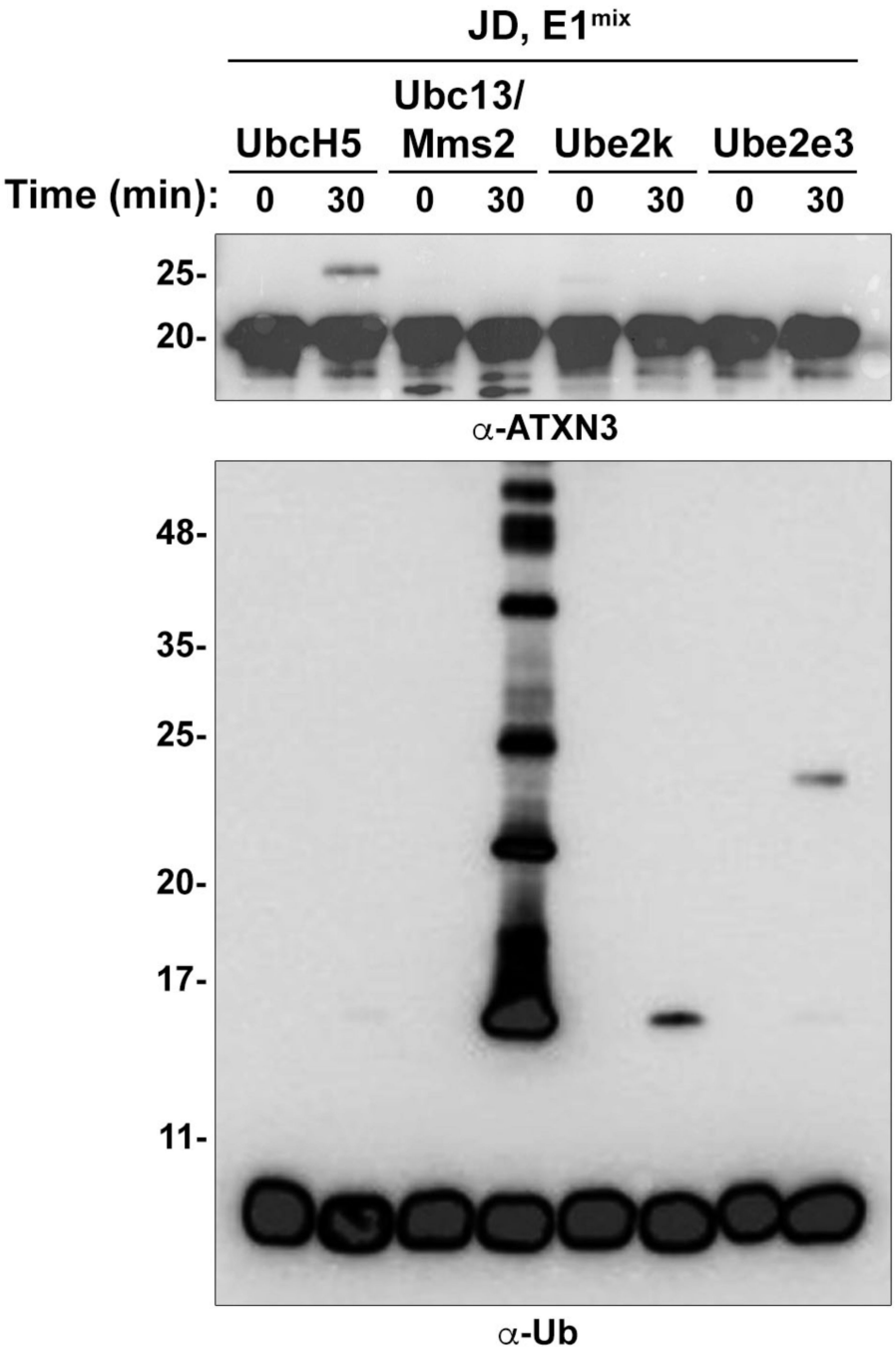

Figure 3: UbcH5, but not other E2s, ubiquitinates the JD of ATXN3 in the absence of CHIP.
E3 independent ubiquitination assays were performed utilizing the JD of ATXN3 were performed with either UbcH5, Ubc13/Mms2, Ube2k, or Ube2e3 as the E2. Samples were analyzed by Western blot with the indicated antibodies.

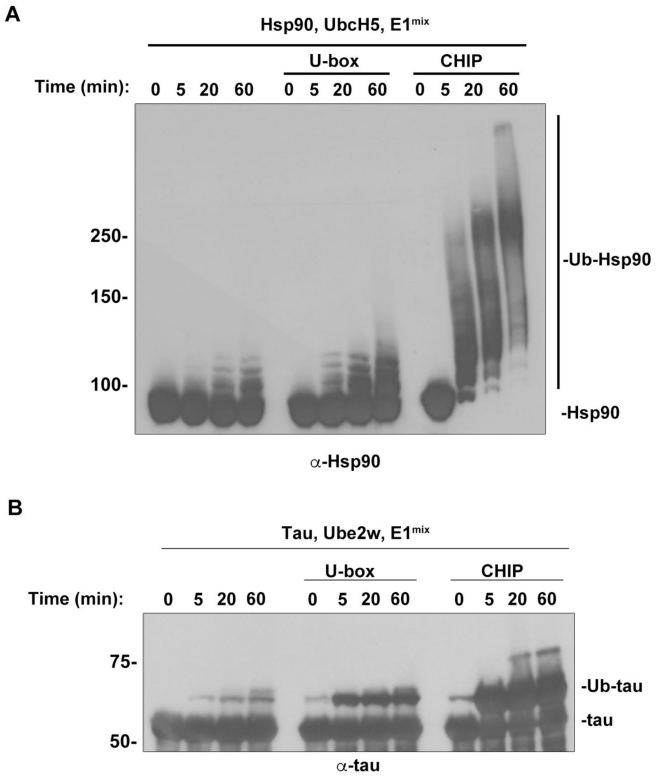

Figure 4. CHIP stimulates ubiquitination through two mechanisms.

A, Hsp90 ubiquitination assays were performed with UbcH5 either alone, in the presence of CHIP's U-box, or in the presence of full-length CHIP. Samples were analyzed by immunoblotting with the indicated antibodies. *B,* Same as in (A) except Ube2w and tau were used in the place of UbcH5 and Hsp90.

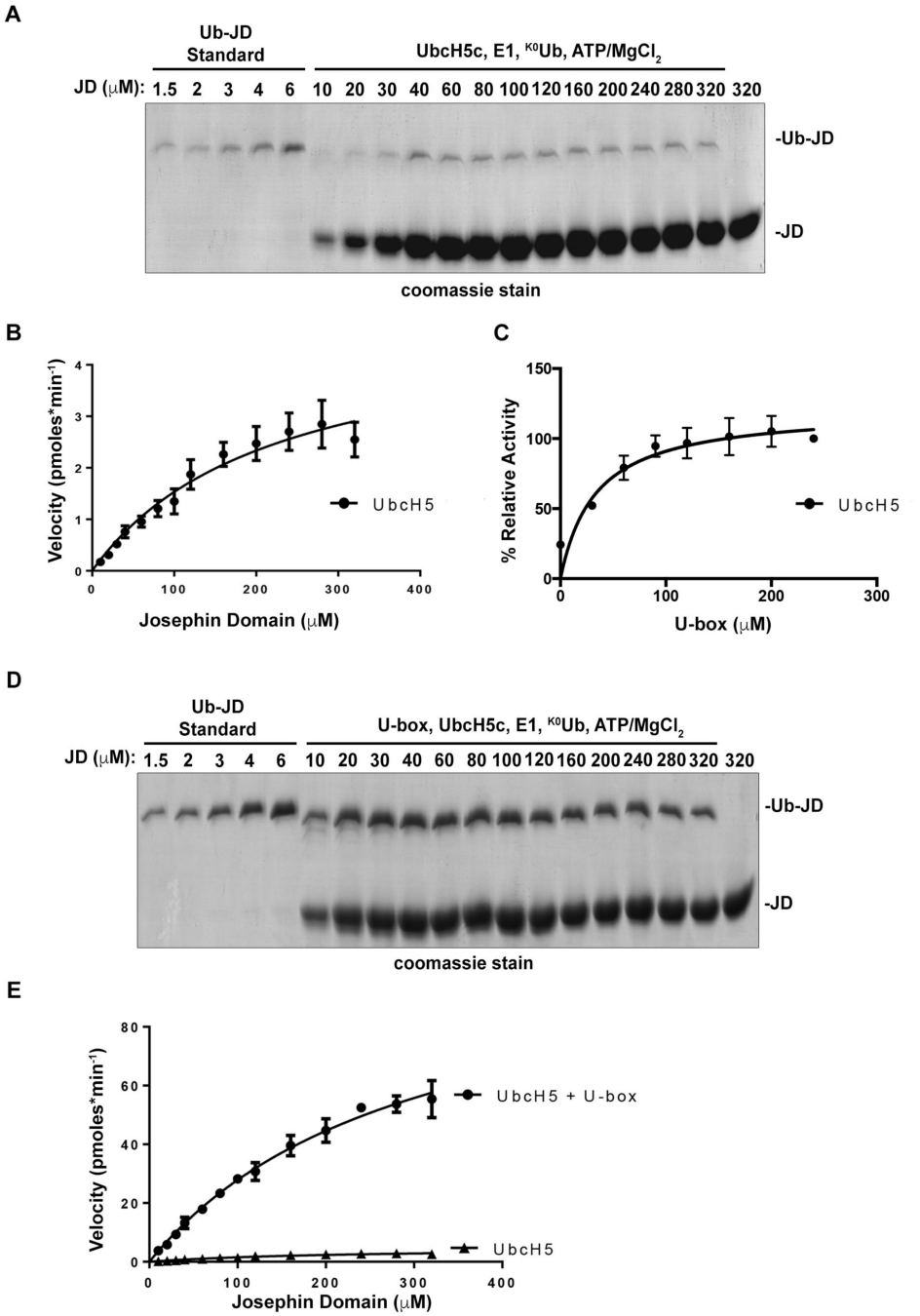

Figure 5. Kinetic characterization of ubiquitination of JD by UbcH5.

A, Ubiquitination assays were performed with 5μM UbcH5c and the indicated concentrations of JD. Samples were loaded as described in experimental methods and were visualized by Coomassie blue. *B,* Ubiquitination assays were quantified from (A) using densitometry to compare the amount of ubiquitinated JD in each lane to a quantified set of monoubiquitinated JD standards in lanes 1–5. *C,* Determination of the amount of U-box required to maximally stimulate UbcH5 activity. JD ubiquitination assays were performed with 5μM UbcH5 and increasing concentrations of CHIP's U-box domain and analyzed by

Coomassie stain. Images were quantified using ImageJ. *D,* Kinetic characterization of UbcH5 activity in the presence of CHIP's U-box. Ubiquitination assays were performed as in (A) with increasing concentrations of JD as a substrate, using 5μM UbcH5c and 200μM of CHIP's U-box domain. Reactions were visualized by Coomassie blue. *E,* Comparison of the initial reaction velocities from ubiquitination assays performed in (A) and (D).

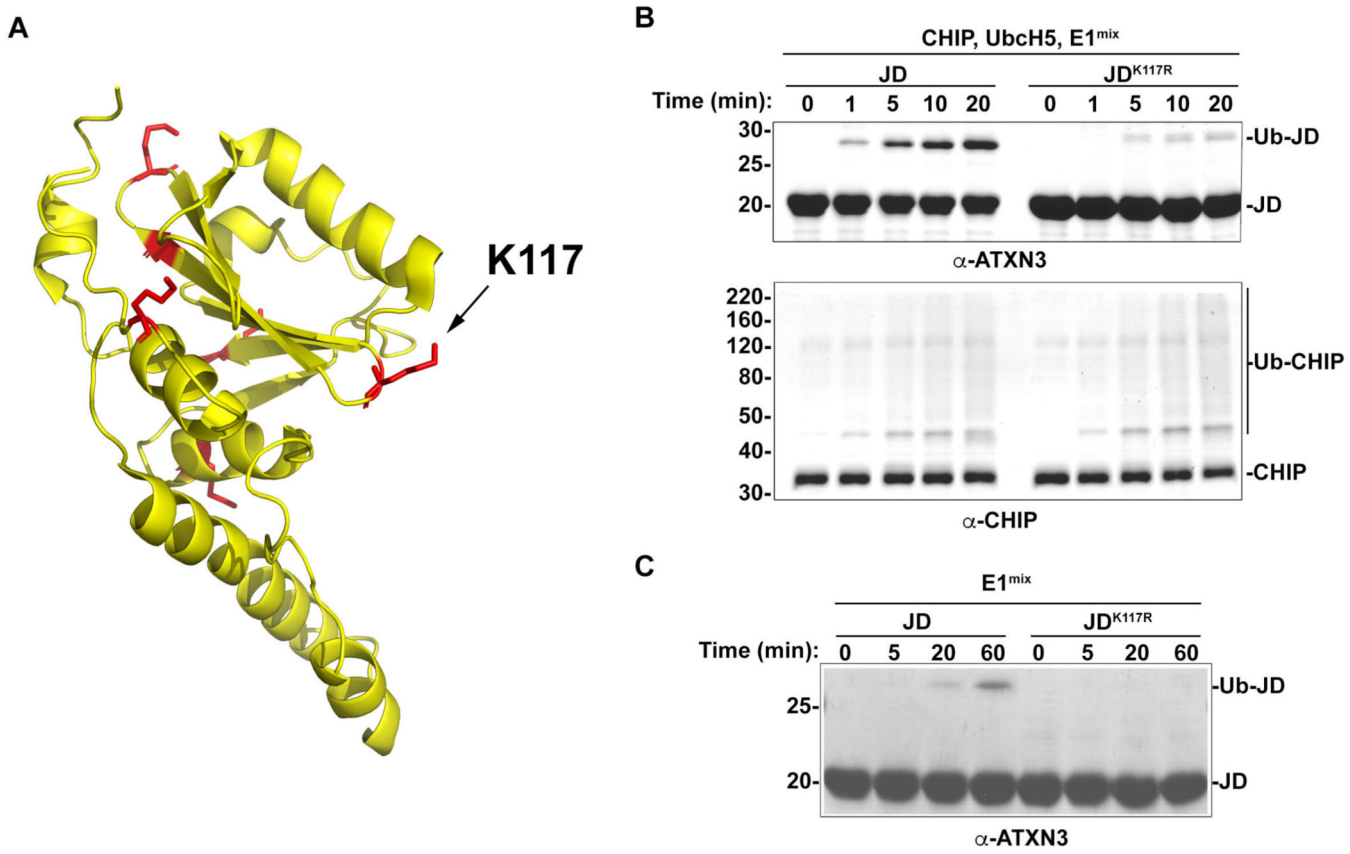

Figure 6. UbcH5 identifies substrate lysine in the absence of CHIP.

A, JD (PDB ID: 1YZB) with surface exposed lysines residues (red). *B,* Ubiquitination assays were performed using 1μM JD or JD^{K117R} in the presence of 1μM CHIP and 1μM UbcH5 and analyzed by immunoblotting with the indicated antibodies. *C,* UbcH5 preferentially ubiquitinates JD K117 in the absence of CHIP. Ubiquitination reactions using 20μM JD or JD^{K117R} were performed with 5μM UbcH5 and analyzed by Coomassie stain.

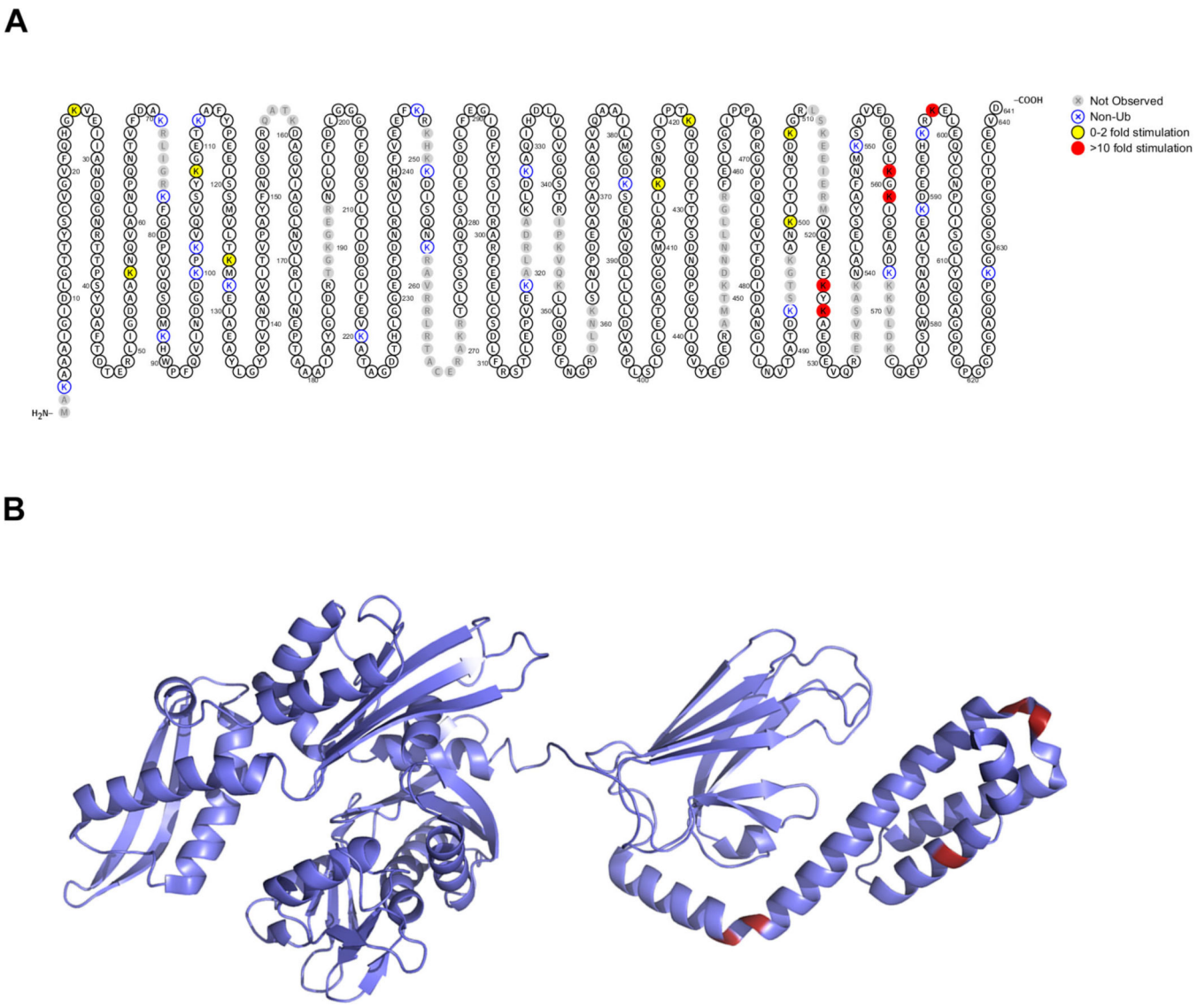

Figure 7. UbcH5 ubiquitinates the same subset of lysines in the absence of CHIP and CHIP stimulates the ubiquitination of a subset of these residues.

A, UbcH5 ubiquitinates the same lysines subset in the presence and absence of CHIP, but CHIP impacts the frequency that a subset of substrate lysines become ubiquitinated. Primary amino acid sequence of Hsp70 showing quantification of ubiquitination at each lysine, presented as a ratio of fold-increase in Hsp70 ubiquitination by UbcH5c in the presence of CHIP. *B*, Ubiquitination of Hsp70 residues that CHIP stimulated by greater than 10-fold (K524, K526, K559, K561, and K597) are shown superimposed on the structure of the Hsp70 homologue, DNAK (PDB ID: 2KHO).

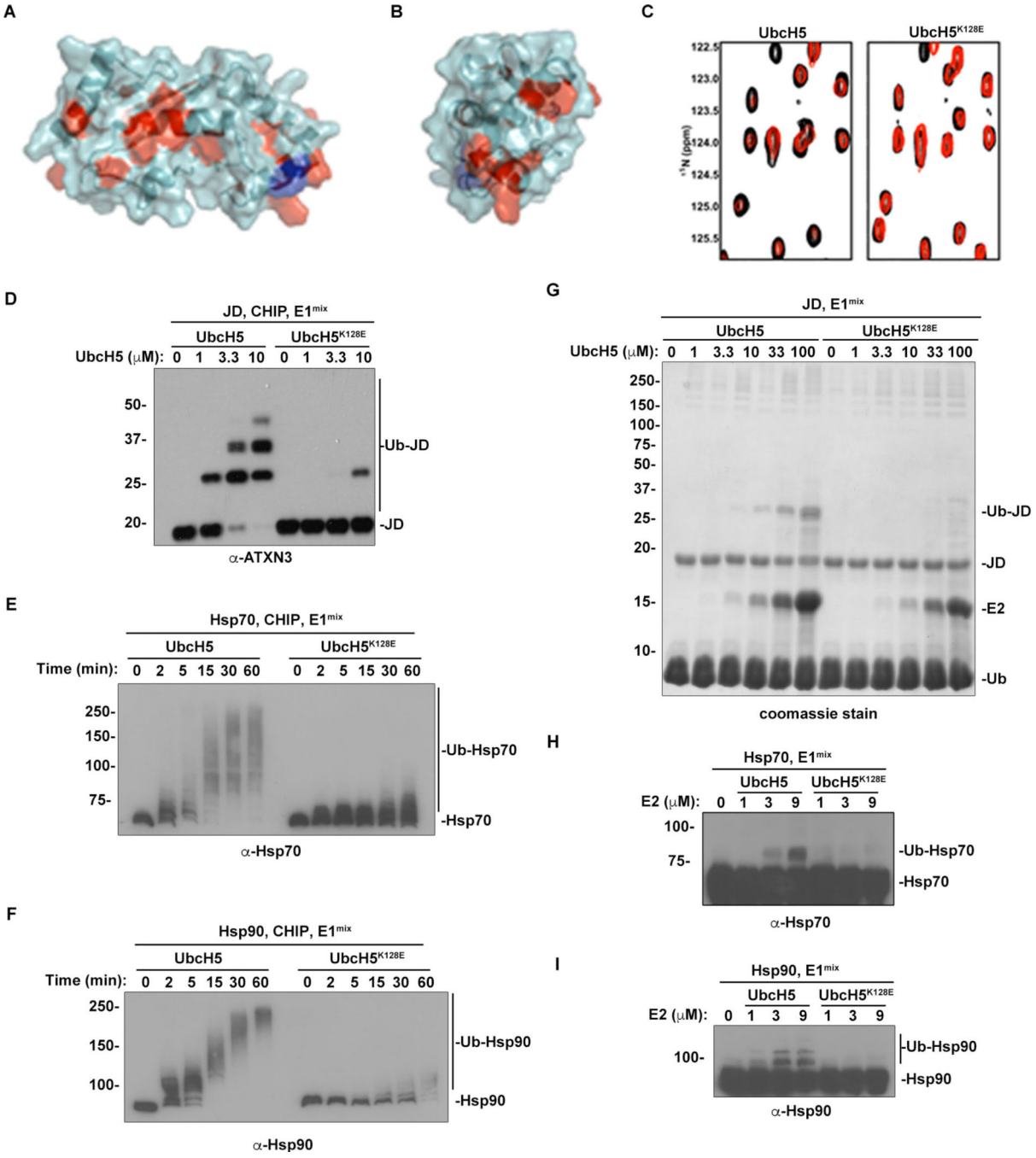

Figure 8. Identification of a substrate binding surface on UbcH5.

A,B, Hsp70 binds UbcH5 in the absence of CHIP. Residues of UbcH5c demonstrating perturbations upon addition of substrate are indicated (red) including K128 (blue) on the structure of U(PDB ID: 2FUH). *C,* The K128E mutation disrupts the UbcH5/Hsp70 interaction. ^{15}N-HSQC spectra of UbcH5c alone (red) or in the bcH5c presence of Hsp70 (black). Results are shown for UbcH5c (left) and UbcH5c^{K128E} (right). *D,* The K128E mutation disrupts the CHIP dependent ubiquitination of JD. JD ubiquitination assays were performed with 1μM JD and the indicated concentrations of either UbcH5c or

UbcH5c^{K128E}. Samples were analyzed by immunoblotting with anti-ATXN3 antibody. *E,* The K128E mutation disrupts the CHIP dependent ubiquitination of Hsp70. Hsp70 ubiquitination assays were performed with 1μM Hsp70 and 1μM UbcH5 or UbcH5^{K128E} for the time points indicated. Samples were analyzed by immunoblotting with anti-Hsp70 antibody. *F,* Same as in E except Hsp90 was used in place of Hsp70. *G,* The K128E mutation disrupts the CHIP independent ubiquitination of JD. JD ubiquitination assays were performed with 20μM JD and the indicated concentrations of either UbcH5c or UbcH5c^{K128E}. Samples were analyzed by Coomassie stain. *H,* Same as in (G) with Hsp70 as the substrate. *I,* Same as in (H) with Hsp90 as the substrate.

Table 1:

K_M and Vmax values for the transfer of lysine-less ubiquitin from UbcH5 to JD^{K117} in the absence and presence of saturating concentrations of CHIP's U-box domain.

	K_m (μM)	V_{MAX}(pmol*min−1)	k_{cat}(min−1)	K_M/k_{cat}(M−1min−1)
UbcH5	220.3 ± 67.8	4.9 ±0.8	0.98 ±0.16	2.25×10^{-4}
UbcH5 + U-box	301.4 ±34.5	111.8 ±7.7	22.35 ±1.54	1.35×10^{-5}